energies

MDPI

Article

Performance Analysis of the Coupled Heating System of the Air-Source Heat Pump, the Energy Accumulator and the Water-Source Heat Pump

Wenhe Zhou *, Bin Wang, Meng Wang and Yuying Chen

School of Environmental and Municipal Engineering, Lanzhou Jiaotong University, Lanzhou 730070, China
* Correspondence: zwh6888@mail.lzjtu.cn

Abstract: In the remote areas of northern China without central heating and gas supply, for users intending to replace coal-boilers, the air-source heat pump system is always questionable due to the contradiction between its heating capacity and user's heating demand, especially in very cold areas, whose *COP* and economy is very poor. The accumulator with phase change materials would be a promising one to solve this problem. With the help of TRNSYS software, a heating system coupled with air-source heat pump, accumulator, and water-source heat pump and its operation mode are provided and analyzed based on the heat source renovation demand of a middle school in Tianshui City suburb which has 5560 m^2 area to be heated. The average *COP* simulated during the heating period of the coupled heating system is 2.23. Based on the simulation model and results, the heat source renovation of the middle school in Tianshui City suburb was carried out, its tested and simulated *COP* over the day was 2 and 2.05, respectively, which also reveals the validity of the numerical method for this problem.

Keywords: heating system; air-source heat pump; energy accumulator

check for updates

Citation: Zhou, W.; Wang, B.; Wang, M.; Chen, Y. Performance Analysis of the Coupled Heating System of the Air-Source Heat Pump, the Energy Accumulator and the Water-Source Heat Pump. *Energies* **2022**, *15*, 7305. https://doi.org/10.3390/en15197305

Academic Editor: Adrián Mota Babiloni

Received: 2 September 2022
Accepted: 29 September 2022
Published: 4 October 2022

Publisher's Note: MDPI stays neutral with regard to jurisdictional claims in published maps and institutional affiliations.

Copyright: © 2022 by the authors. Licensee MDPI, Basel, Switzerland. This article is an open access article distributed under the terms and conditions of the Creative Commons Attribution (CC BY) license (https://creativecommons.org/licenses/by/4.0/).

1. Introduction

Building energy consumption has accounted for one-third of the terminal energy consumption and is expected to reach 40% by 2030 in China [1,2], of which the energy consumption for heating, ventilation, and air conditioning (HVAC) account for 50% [3]. China is struggling to cut carbon emissions in each field [4] and a heating system based on coal-boilers will be prohibited in coming years. Located in the suburb of 35° N and 106° E, the middle school in Tianshui City suburb is very cold and was encouraged by government to replace the heating coal-boiler with equipment in clean energy. However, its gas supply and central heating are blank, and the transformation fund is insufficient for a geothermal heat pump. The same problem is facing many users in northern China [5–7].

Heat pumps are often recommended as an alternative to coal-boilers for clean heating [8–11]. A geothermal heat pump is efficient and stable at the initial stage, but its initial investment for well drilling is too high for some users to be able to afford it and its performance would deteriorate gradually [12–15]. The advantages of air-source heat pump (ASHP) include easy installation and lower initial investment [16–21], but it would be uneconomical in cold areas, and it's defrost is another fatal flaw [22–26]. What type of heat pump is suitable for the users such as the school in Tianshui City suburb?

Wei Wang et al. combined ASHP and water-source heat pump (WSHP) for heating in a low-temperature environment [27]. Xu studied the performance of the two-stage heat pump in cold areas [28]. Lin et al. proposed an ASHP system combined with a latent heat storage unit [29]. Qu manufactured an ASHP energy storage system prototype, and tested it at various operating modes [30]. Redon et al. conducted parameter optimization and theoretical research on dynamic operation characteristics of a two-stage compression ASHP system with different refrigerants [31]. Chen et al. studied a new solar-assisted heat pump

system with phase-change energy storage function, established a numerical model of key parts, and experimentally met the cold-day heating demand in rural areas of Yanbian City, Jilin Province, China [32]. Zhang et al. proposed a novel solar photovoltaic/heat-assisted gas engine-driven energy storage heat pump system, and studied the obtained independent variables (solar radiation, outdoor dry bulb temperature and wind speed) and dependent variables (building heating load, SESGEHP heating capacity, heat gain and power generation from PV/T systems) [33]. Seevers J.-P. establish a numerical model of a heat pump and storage system using the Monte Carlo method. Results show that relatively small heat pumps and energy storage can ensure reliable heating and cooling of manufacturing systems [34]. The energy efficiency of the heating system was improved when the phase change accumulator was introduced [35–38].

It is clear that the clean heating is difficult to implement in the poor and remote areas. As one promising solution, a heating system coupled with ASHP, heat accumulator, and WSHP has been little discussed. To satisfy the heating demand of the users such as the middle school in Tianshui City suburb, this paper proposes a coupled heating system. Then, a numerical analysis by TRNSYS software is followed to indicate the system performance. Finally, the practical effect of the coupled heating system is shown.

2. The Project Background

The heating period is from 16 November to 31 March of the following year in Tianshui city, but for the school, the period could be from 16 November to 20 January of the following year and 1 March to 31 March. The outdoor design temperature for heating is −7 °C and the indoor design temperature for heating is 18 °C during the occupied period. Figure 1 shows the hourly outdoor temperature of a typical meteorological year in Tianshui city recorded in ASHRAE (American Society of HVAC Engineers) database [39], in which the highest temperature, the lowest temperature, and the average temperature are 23.5 °C, −9.3 °C, and 1.4 °C, respectively. The conditioned area of the middle school is 5560 m^2 and Figure 2 shows its regional layout. In order to cater to the national goal of carbon reduction, the middle school aims to transform the coal-boiler system into a heat pump system based on the existing pipe network and radiators due to lack of natural gas and central heating, but the transform fund is insufficient. The question of whether the heating system based on ASHP is practical has arisen for the middle school, and numerical prediction could be necessary.

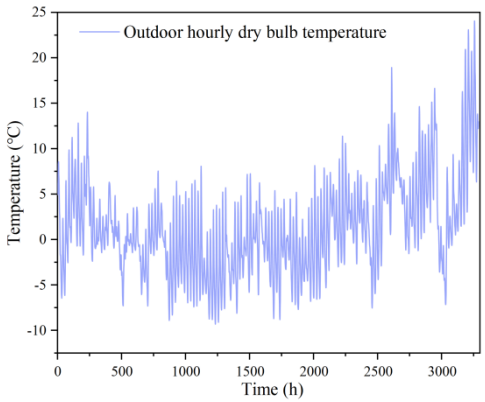


Figure 1. Hourly outdoor temperature.

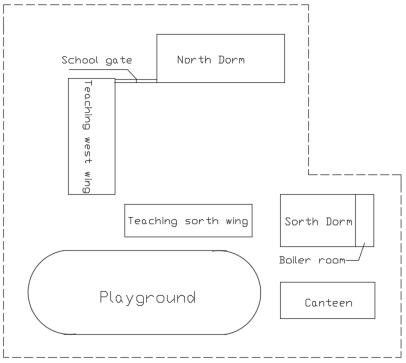


Figure 2. Regional layout of the school.

Figure 3 shows the predesigned heat pump system, which is mainly composed of 9—ASHP at low temperature side, 8—the middle part of energy accumulator, and 6—WSHP at high temperature side. Other sections include 1—make-up water, 2—make-up pump, 3—circulating pump for heating, 4—return water of heating, 5—supply water of heating, 7—circulating pump at WSHP evaporator side and 10—make-up water tank. R410a and R134a are used as the refrigerants for ASHP and WSHP, respectively.

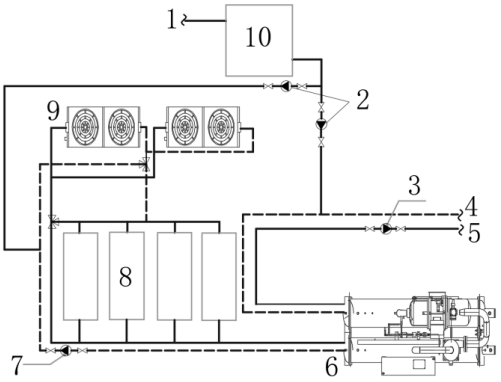


Figure 3. The heat pump heating system.

The operation mode for the heating system is the key factor of its component capacities and its energy and cost. In Gansu province, the peak and valley electricity price policy is implemented, and it will be counted at the valley electricity price at 10:00 p.m. to 8:00 a.m. when the user uses clean and renewable energy. Considering improving the *COP* of ASHP and the peak and valley electricity price policy, the operation mode for the heating system proposed in this paper mainly includes four stages shown as Table 1. During stage 1, ASHP supplies 17–25 °C water to energy accumulator and WSHP evaporator simultaneously, then, the WSHP condenser supplies about 55 °C water to the buildings. During stage 2, the ASHP stops, the accumulator supplies warm water to the WSHP, and the WSHP heats the buildings. The process in stage 3 and stage 4 are the same as that in the stage 1 and stage 2 respectively. Whenever the heat capacity of the accumulator is less than the demanded heating load, the ASHP will put into operation.

Table 1. Operation strategy.

Model	ASHP	Accumulator	WSHP	Period
1	working	Heat recharge	working	10:00 a.m.–6:00 p.m.
2	stop	Heat release	working	6:00 p.m.–10:00 p.m.
3	working	Heat recharge	working	10:00 p.m.–6:00 a.m.
4	stop	Heat release	working	6:00 a.m.–10:00 a.m.

3. Simulation Analysis

3.1. Evaluation Index

COP shown in Equation (1) is used to evaluate the energy efficiency of the heat pump and its system.

$$COP = \frac{\dot{Q}}{P_{h_p} + \sum P_p} \quad (1)$$

where, P_{hp} is the power consumption of the heat pump. P_p is the power consumption of the water pump, and it is equal to zero when *COP* is for the heat pump only. $\dot{Q}$ is the heating capacity of the heat pump, and it is the heating capacity of WSHP when the *COP* is for the heating system. $\dot{Q}$ can be calculated according to Equation (2).

$$\dot{Q} = \dot{m} c_p (t_2 - t_1) \quad (2)$$

where, $\dot{m}$ is the mass flow rate. c_p is specific heat capacity of water. t_1 and t_2 are the water temperature at inlet and outlet of the heat pump or the heating system, respectively.

3.2. Heating Load and Component Capacity

Based on the building information of the school and the meteorological data of the typical year in ASHRAE database, the school hourly heating load is calculated by OpenStudio software (Golden, USA) and shown in Figure 4. The maximum heating load is 353.3 kW and the average heating load is 253.72 kW. The designed load for heating the school is 325.4 kW according to the design parameters, which should be satisfied by the WSHP. If the accumulator spends 8 h in thermal storing and 4 h in thermal releasing, the accumulator capacity should be larger than 976.2 kWh and the ASHP heating capacity should be larger than 366.1 kW. If the factor 1.2 is considered for the capacity redundancy of the system, the main equipment and their parameters are determined as Table 2 shown.

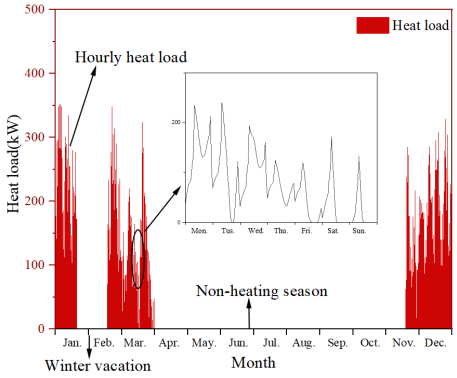


Figure 4. Heat load during heating period.

Table 2. Main equipment and their parameters.

No.	Device Name	Parameter	Quantity
1	WSHP	max heating capacity: 390 kW, max input power: 80 kW	1
2	ASHP 1	max heating capacity: 300 kW, max input power: 120 kW	1
3	ASHP 2	max heating capacity: 150 kW, max input power: 60 kW	1
4	circulating pump of ASHP	rated input power: 10 kW	2
5	circulating pump of WSHP	rated input power: 10 kW	2
6	accumulator	capacity:293 kW	4

3.3. System Simulation Model

The simulated system shown in Figure 5 will be used to analyze the performance of the system, which is developed in TRNSYS 16.0 software (Ouagadougou, Burkina Faso). The model includes key components, such as the ASHP, WSHP, accumulator, several pumps, and the pipeline. Numerical model includes the formulas established by reference [40]. Each operating parameter of the heating system is monitored in real time.

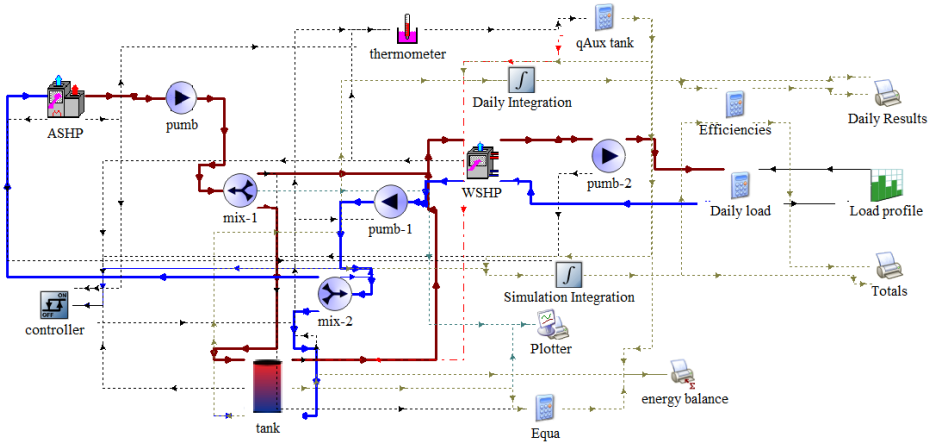


Figure 5. The simulated model.

3.4. Numerical Results and Analysis

In order to numerically analyze the hourly heating capacity, Figure 6a,b give the hourly utilization coefficients of different rooms to consider the heat obtained from the human body and electrical equipment along each day respectively, including the classroom, the office, the dining room and the dormitory.

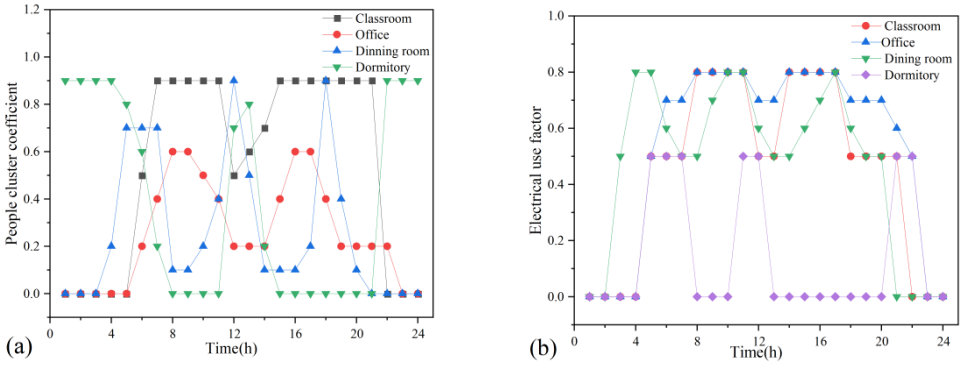


Figure 6. Hourly utilization coefficient (**a**) for people, (**b**) for electrical equipment.

As the known conditions, the outdoor ambient temperature, the water temperatures at ASHP condenser inlet, and WSHP evaporator inlet and WSHP condenser outlet (i.e., the water temperature for heating users) are input. The phase change temperature in the accumulator is set to 20 °C.

3.4.1. COPs Simulated in the Heating Period

Figure 7 shows the hourly *COP* of the WSHP, the ASHP, and the coupled heating system (including water pumps and heat pumps) simulated during the heating season, except for winter vacation. The WSHP *COP* is stable during heating period and its average value is 3.9. The ASHP *COP* fluctuates with outdoor temperature and its average value is 2.33. A small fluctuation of *COP* of the coupled heating system is caused by ASHP and its average value is 2.2. The result could be satisfied compared to the heating system composed by ASHP only, whose *COP* is usually far less than 2.0 during cold period.

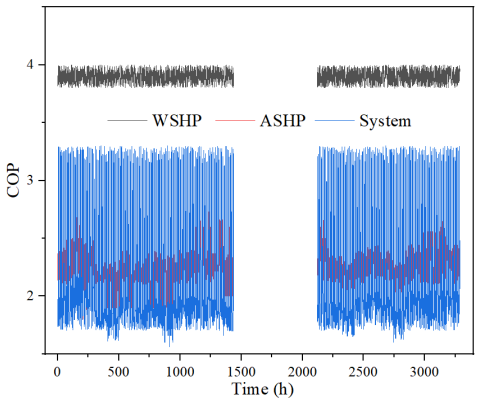


Figure 7. The hourly *COP*s during heating period.

3.4.2. Benefit Predict

Based on the meteorological parameters of typical year and operation mode in this paper, annual energy consumption of the coupled heating system provided by this paper is about 223,164 kWh, of which, 53.14% belongs to ASHP and 43.4% to WSHP. Because the working time of the coupled heating system was 22:00 p.m. to 8:00 a.m., it will be counted at the valley electricity price (about 50%), which is ¥0.32 ($0.046)/kWh (¥0.54 ($0.077)/kWh in rest time). The operating costs for heating during heating period is about ¥105,330 ($15,021.61) total or ¥18.9 ($2.70)/(y·m^2), which is a lower level in China.

4. The Project

Based on the above simulation analysis, the heating system was put into practice in the middle school in 2019. The system and its main equipment was run according to the mode shown in Table 1. The WSHP can automatically adjust working power level to 60 kW or 75 kW according to the heating water temperature, and ASHP1 can automatically adjust total working power level to 90 kW or 120 kW according to environment temperature. The tested parameters and instruments are shown in Table 3.

Table 3. Test parameters and instruments.

Parameters	Instruments	Types	Accuracy	Quantity
Outdoor temperature	Thermometer	LGR-WD01u	±0.2–0.5 °C	1
	Thermal resistance sensor	WZP-230	PT100, Level A	1
Indoor temperature	Thermometer	LGR-WD01u	±0.2–0.5 °C	6
Flow rate and water temperature	Ultrasound calorimeter (temperature probe and flow probe)	TDS-100	2–3%	6
		TDS-100	2–3%	
Power consumption	Smarter meter	CHTK900E-3S4	1 W	1

4.1. Outdoor Temperature and Heating Load

The test was carried out in the same year before vacation. Due to its low temperature, 11 January was selected as the typical day to specifically indicate the performance of the coupled heating system and the validity of the numerical model and method. Figure 8 shows the outdoor temperature of the typical day and the corresponding heating load, which is inversely proportional. The heating load is a little delayed compared to the outside temperature. The highest and lowest outdoor temperatures are 0.8 °C and –8.2 °C respectively. The maximum heating load of the typical day is 368.4 kW at 9 o'clock, which is larger than the designed load for heating school (325.4 kW), and the average heating load is 281.6 kW.

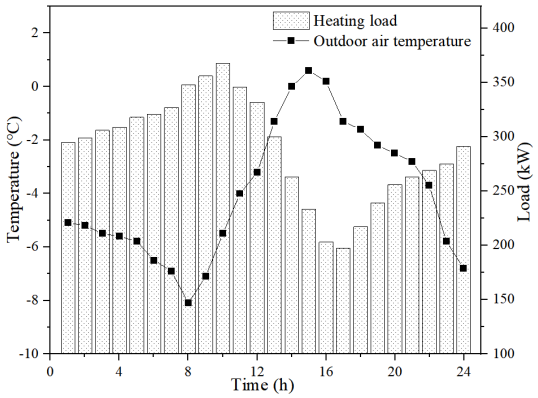


Figure 8. Heating load on typical day.

4.2. Water Temperature at Each Node

Figure 9a,b give the water temperatures simulated and tested at five nodes of the system along the typical day, respectively. Tested results show that the phase transition temperature in the accumulator is 17–21 °C, which is some deviation from 20 °C set in the simulation.

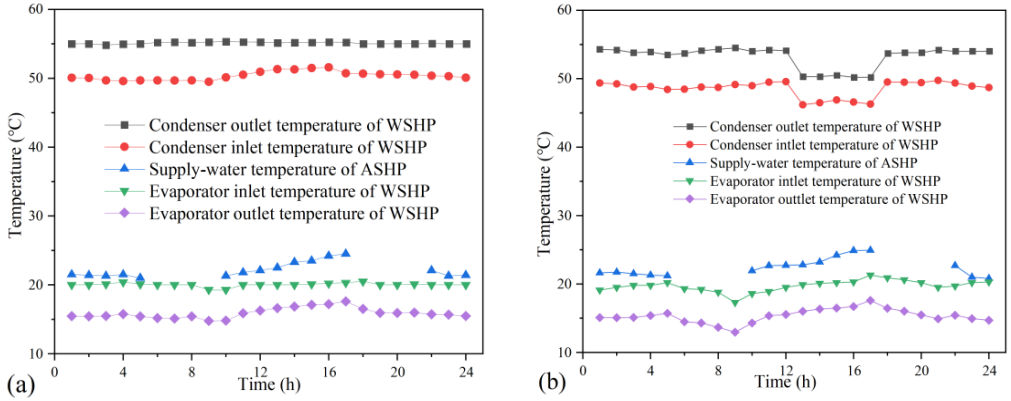


Figure 9. Water temperatures (**a**) simulated, (**b**) tested.

In the simulation, the water temperature at the WSHP condenser outlet to users is 55 °C, and that at the WSHP condenser inlet returning from users is 49.4–51.5 °C depending on the outdoor temperature. Tested results show that the water temperature supplying users is stable and always about 54 °C, except for the afternoon (about 50.5 °C) when the WSHP runs at a lower level automatically, which is similar to the results simulated.

In the simulation, according to the operation strategy in Section 2, the water temperature at ASHP condenser outlet to WSHP evaporator is always higher than 20 °C, even when the ASHP stops, whose average value is 23.4 °C during the working period. The average water temperature at WSHP evaporator outlet to ASHP condenser is 16 °C. Tested results show that the average water temperature at ASHP condenser outlet to WSHP evaporator is about 22.8 °C during the ASHP working period and the water temperature at the WSHP evaporator inlet fluctuates between 18–21 °C. The heat loss along the pipeline leads to a gap between the water temperature at ASHP condenser outlet to WSHP evaporator and that at WSHP evaporator inlet.

4.3. Power Consumed

Figure 10a shows the simulated operating power of the ASHP, the WSHP and the system along the typical day, whose average values are 131.6 kW, 73.8 kW, and 168.5 kW, respectively. Figure 10b shows the power consumption tested of the ASHP, the WSHP, and the system, whose average values are 142 kW, 72 kW, and 188 kW respectively. Both

simulated results and tested results are very similar, and as the outdoor temperature rises, the operating power of WSHP is reduced due to the lower heating demand and the improved ASHP performance. Some deviations between simulation and test could be because some disadvantage factors on the system performance are neglected in the simulation, such as ASHP frost. Here, the system operating power consumed includes the ASHP, WSHP, and water pumps located in the heat source house.

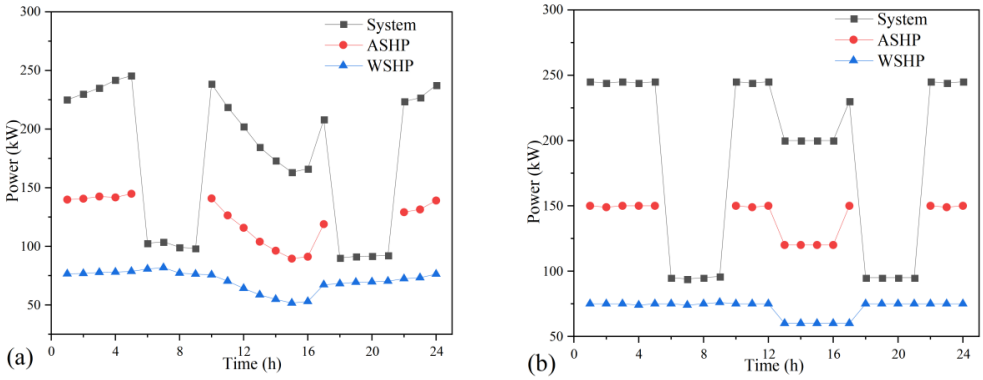


Figure 10. Power of ASHP, WSHP and system. (**a**) simulated, (**b**) tested.

4.4. COPs

Figure 11 gives *COP*s simulated and tested over a the typical day. *COP*s are inversely proportional to corresponding powers consumed. Figure 11a shows the simulated *COP*s of the ASHP, the WSHP, and the system over a typical day, whose average values are 2.38, 3.82, and 2.05, respectively. Figure 11b shows the tested *COP*s over a typical day. The ASHP *COP* is 1.97–2.41 with the outdoor temperature. Because of the fluctuation of the inlet water temperature of the WSHP evaporator and the heating load along the test day, the maximum WSHP *COP* is 3.99 at 8:00 a.m. and the minimum is 3.58 at 12:00 p.m. When the ASHP stops, the system *COP* is larger than 3.3 during 6:00–10:00 a.m. and 3.0 during 6:00–10:00 p.m. The average value of the system *COP* is 2.0.

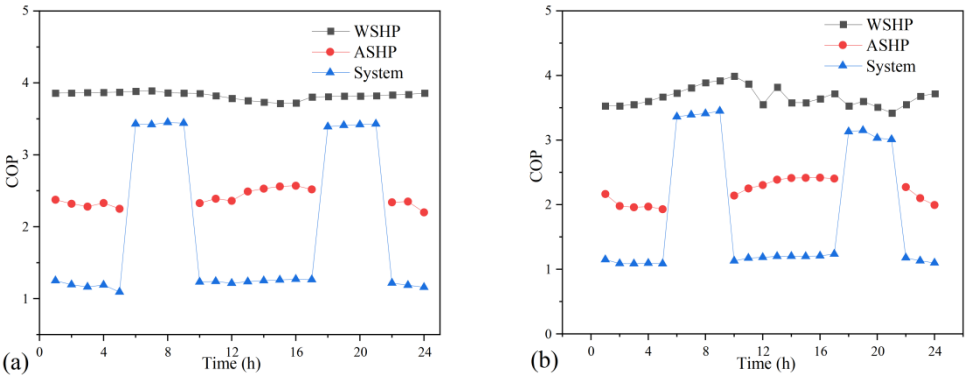


Figure 11. *COP*s of the ASHP, the WSHP, and the system: (**a**) simulated, (**b**) tested.

It is clear that the *COP*s of the ASHP and the system are improved a lot because the accumulators are introduced, and resulting in operating cost saving as well. The simulated results and the tested results are similar.

4.5. Comparison between Numerical Results with Test

In order to illustrate reliability of the simulation method, Figure 12 shows the comparison between the numerical results with corresponding average values tested. Because some disadvantage factors on performance are neglected in the simulation, such as ASHP frost and the input simulated powers changing with the load, there are some gaps between the simulation and the test. The maximum relative error occurs in the power consumed by

the system, which is 9.67%. The relative errors of powers consumed by ASHP and WSHP are 7.5% and 2.78%, respectively. The relative error of ASHP *COP* is 8.67%. The relative error of the WSHP *COP* and the system *COP* are 6.7% and 2.5% respectively. It is clear that the results and analysis based on the numerical model and method could be credible.

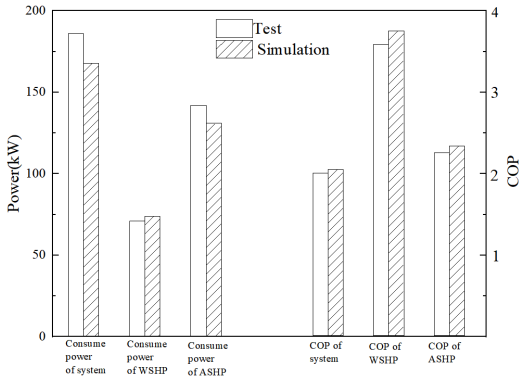


Figure 12. Comparison between simulation and test.

In order to illustrate the heating effect of the system, five rooms in different buildings were selected as the typical rooms and their indoor temperatures were tested over a typical day. Figure 13 shows the tested results and the average temperatures of the five typical rooms were 19.0 °C, 20.9 °C, 19.4 °C, 20.4 °C, 20.5 °C, and 18.2 °C, which indicates the heating system effect.

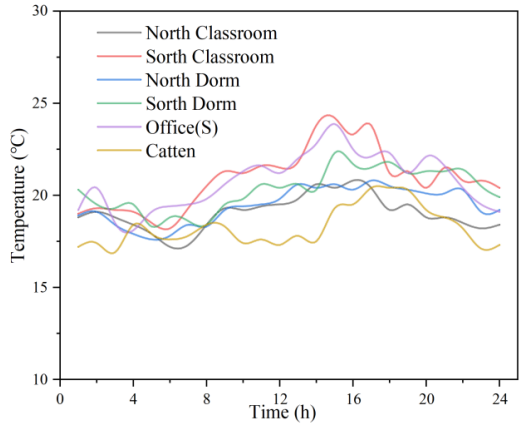


Figure 13. Indoor temperatures in the tested room.

5. Conclusions

By introducing an accumulator, this article innovatively provides a heating system coupled with ASHP, accumulator and WSHP, and the system performance was numerically predicted with the help of TRANSYS software, which was verified by the field test that followed. The conclusions can be drawn as follows:

(1) The numerical model and method developed in TRANSYS is practical and validated to calculate the performance of the heating system, even the coupled heat pump system.
(2) Compared to the ASHP and WSHP system, the initial investment, energy and running cost saving effect of the coupled heating system is significantly improved by the introduced accumulator.
(3) The heating system provided would be the promising one to cater to the clean transformation demand for some users such as the middle school mentioned in this paper.

Author Contributions: Conceptualization, methodology, and writing—review and editing, W.Z.; software, investigation, and writing—original draft preparation B.W.; validation and formal analysis, M.W.; data curation, Y.C. All authors have read and agreed to the published version of the manuscript.

Funding: This research was funded by Gansu Provincial Department of Education: Excellent Postgraduate "Innovation Star" Project grant number 2022CXZX-560.

Institutional Review Board Statement: Not applicable.

Informed Consent Statement: Not applicable.

Conflicts of Interest: The authors declare no conflict of interest.

References

1. Abduljalil, A.; Al, A.; Mat, S.B.; Sopian, K.; Sulaiman, M.Y.; Lim, C.H.; Abdulrahman, T. Review of thermal energy storage for air conditioning systems. *Renew Sust. Energ. Rev.* **2012**, *16*, 5802–5819.
2. Wu, Y.F. Investigation and analysis of the status quo and trend of building energy efficiency in China. *Low Carbon World* **2017**, *17*, 151–152.
3. Chua, K.J.; Chou, S.K.; Yang, W.M.; Yan, J. Achieving better energy-efficient air conditioning–A review of technologies and strategies. *Appl Energ.* **2013**, *104*, 87–104. [CrossRef]
4. Jiang, Y. China Building Energy Research Report 2020. *Build. Energy Effic.* **2021**, *49*, 1–6.
5. Chua, K.J.; Chou, S.K.; Yang, W.M. Field test investigation of a double-stage coupled heat pumps heating system for cold regions. *Int. J. Refrig.* **2005**, *28*, 672–679.
6. Ozgener, O.; Hepbasli, A. A review on the energy and exergy analysis of solar assisted heat pump systems. *Renew Sustain. Energy Rev.* **2007**, *11*, 482–496. [CrossRef]
7. Ma, J.F.; Qian, Q.K.; Visscher, H.; Song, K. Homeowners' Participation in Energy Efficient Renovation Projects in China's Northern Heating Region. *Sustainability* **2021**, *13*, 9037. [CrossRef]
8. Wu, Y.; Meng, Q.; Li, L.; Mu, J.Y. Interaction between Sound and Thermal Influences on Patient Comfort in the Hospitals of China's Northern Heating Region. *Appl. Sci.* **2019**, *9*, 5551. [CrossRef]
9. Zheng, Z.H.; Zhou, J.; Xu, F.; Zhang, R.; Guang, D. Integrated operation of PV assisted ground source heat pump and air source heat pump system: Performance analysis and economic optimization. *Energy Convers. Manag.* **2022**, *269*, 116091. [CrossRef]
10. Chen, Q.; Li, N. Energy, emissions, economic analysis of air-source heat pump with radiant heating system in hot-summer and cold-winter zone in China. *Energy Sustain. Dev.* **2022**, *70*, 10–22. [CrossRef]
11. Ermel, C.; Bianchi, M.V.A.; Cardoso, A.P.; Schneider, P.S. Thermal storage integrated into air-source heat pumps to leverage building electrification: A systematic literature review. *Appl. Therm. Eng.* **2022**, *215*, 118975. [CrossRef]
12. Lu, S.L.; Feng, W.; Kong, X.F.; Wu, Y. Analysis and case studies of residential heat metering and energy-efficiency retrofits in China's northern heating region. *Renew Sust. Energy Rev.* **2014**, *38*, 765–774. [CrossRef]
13. Li, S.Y.; Lu, J.; Li, W.Y.; Zhang, Y.Q.; Huang, S.; Tian, L.; Lv, Y.F.; Hu, Y.F.; Zeng, Y.J. Thermodynamic analyses of a novel ejector enhanced dual-temperature air source heat pump cycle with self-defrosting. *Appl. Therm. Eng.* **2022**, *215*, 118944. [CrossRef]
14. Gao, B.; Xiao, Y.Z.; Xiao, J.Y.; Yan, P.Y.; Nan, Y.Y.; Ji, N. Operation performance test and energy efficiency analysis of ground-source heat pump systems. *J. Build. Eng.* **2021**, *41*, 102446. [CrossRef]
15. Shi, F.H. ASHP Technology and Application. *HVAC* **2019**, *49*, 86–95.
16. Xu, W.; Liu, C.P.; Li, A.G.; Li, J.; Qiao, B. Feasibility and performance study on hybrid air source heat pump system for ultra-low energy building in severe cold region of China. *Renew. Energy* **2020**, *146*, 2124–2133. [CrossRef]
17. Ling, J.H.; Tong, H.; Xing, J.C.; Zhao, Y.X. Simulation and optimization of the operation strategy of ASHP heating system: A case study in Tianjin. *Energy Build.* **2020**, *226*, 110349. [CrossRef]
18. Li, X.Y. The Theory and Application of Compressor Intermediate Air-supplement Heat Pump Technology for Heating in Severe Cold Regions of Inner Mongolia. *J. Beijing Jiaotong Univ.* **2018**, *42*, 131–136.
19. Meng, Y.; Sheng, L.; Xue, J.Z.; Yang, Z. Techno-economic analysis of air source heat pump combined with latent thermal energy storage applied for space heating in China. *Appl. Therm. Eng.* **2021**, *185*, 116434.
20. Xu, Z.W.; Zhao, W.Y.; Shao, S.Q.; Wang, Z.C.; Xu, W.; Li, H.; Wang, Y.C.; Wang, W.; Yang, Q.; Xu, C. Analysis on key influence factors of air source heat pumps with field monitored data in Beijing. *Sustain. Energy Technol.* **2021**, *48*, 101642. [CrossRef]
21. Sandra, R.L.C.; José, L.B.A. Phase change materials and energy efficiency of buildings: A review of knowledge. *J. Energy Storage* **2020**, *27*, 101083.
22. Mohanrajab, M.; Karthicka, L.; Dhivagar, R. Performance and economic analysis of a heat pump water heater assisted regenerative solar still using latent heat storage. *Appl. Therm. Eng.* **2021**, *196*, 117263. [CrossRef]
23. Badescu, V. Model of a thermal energy storage device integrated into a solar assisted heat pump system for space heating. *Energy Convers. Manag.* **2003**, *44*, 1589–1604. [CrossRef]
24. Lizana, J.; Friedrich, D.; Renaldi, R.; Chacartegui, R. Energy flexible building through smart demand-side management and latent heat storage. *Appl. Energy* **2018**, *230*, 471–485. [CrossRef]
25. Chu, S.; Wei, J.H.; Liu, Q.M. Scheme design and economic analysis of ground-source heat pump composite water storage system with buried pipes. *Build. Energy Effic.* **2020**, *48*, 58–67.

26. Tang, R.; Wang, F.; Wang, Z.H.; Yang, W.W. Division of Frosting Type and Frosting Degree of the Air Source Heat Pump for Heating in China. *Front. Energy Res.* **2021**, *9*, 708478. [CrossRef]
27. Li, Z.Y.; Wang, W.; Sun, Y.Y.; Wang, S.Q.; Shiming, D.; Yao, L. Applying image recognition to frost built-up detection in air source heat pumps. *Energy* **2021**, *2022*, 121004. [CrossRef]
28. Xu, L.F.; Li, E.T.; Xu, Y.J.; Mao, N.; Shen, X.; Wang, X.L. An experimental energy performance investigation and economic analysis on a cascade heat pump for high-temperature water in cold region. *Renew. Energy* **2020**, *152*, 674–683. [CrossRef]
29. Lin, Y.; Fan, Y.B.; Yu, M.; Jiang, L.; Zhang, X.J. Performance investigation on an air source heat pump system with latent heat thermal energy storage. *Energy* **2022**, *239*, 121898. [CrossRef]
30. Qu, D.H. Research on Characteristics of Solar-Assisted ASHP Energy Storage System. Master's Thesis, Harbin Institute of Technology, Harbin, China, 2017.
31. Redón, A.; Navarro-Peris, E.; Pitarch, M.; Gonzálvez-Macia, J.; Corberán, J.M. Analysis and optimization of subcritical two-stage vapor injection heat pump systems. *Appl. Energy* **2014**, *124*, 231–240. [CrossRef]
32. Chen, X.; Yang, H. Performance analysis of a proposed solar assisted ground coupled heat pump system. *Appl. Energy* **2012**, *97*, 888–896. [CrossRef]
33. Zhang, J.M.; Yang, H.; Luo, D.W. The operation strategy of the combined system of ground-source heat pump and water storage is redesigned. *Gas Heat* **2019**, *39*, 15–25.
34. Seevers, J.P.; Schlosser, F. Integration of heat pump storage systems in manufacturing systems via data farming and Monte Carlo simulation. *Chem. Eng. Trans.* **2019**, *76*, 373–378.
35. Hirmiz, R.; Teamah, H.M.; Lightstone, M.F.; Cotton, J.S. Performance of heat pump integrated phase change material thermal storage for electric load shifting in building demand side management. *Energy Build.* **2019**, *190*, 103–118. [CrossRef]
36. Chen, H.F.; Li, G.Q.; Ling, Y.Y.; Fu, J.; Wang, Y.J.; Yang, J.; Jiang, L.Y.; Badiei, A.; Zhang, Y. Experimental Analysis of a Solar Energy Storage Heat Pump System. *J. Therm. Sci.* **2021**, *30*, 1491–1502. [CrossRef]
37. Zhang, Q.; Zhao, Y.; Li, N.; Feng, F.; Shi, P.F. A novel solar photovoltaic/thermal assisted gas engine driven energy storage heat pump system (SESGEHPs) and its performance analysis. *Energy Convers. Manag.* **2019**, *184*, 301–314. [CrossRef]
38. Christoph, Z.; Bernd, W.; Michael, L.; Gerwin, D.S. Thomas Leitgeb. Development of an Energy Efficient Extrusion Factory employing a latent heat storage and a high temperature heat pump. *Appl. Energy* **2020**, *259*, 114114.
39. American Society of Heating; Refrigerating and Air-Conditioning Engineers; US Green Building Council; National Association of Home Builders of the United States. *National Green Building Standard: ANSI/ASHRAE/NAHB/ICC Standard ICC/ASHRAE 700-2015*; National Association of Home Builders of the United States: Washington, DC, USA, 2016; pp. 1–76.
40. Wang, Y.B.; Quan, Z.H.; Jing, H.R.; Wang, L.C.; Zhao, Y.H. Performance and operation strategy optimization of a new dual-source building energy supply system with heat pumps and energy storage. *Energy Convers. Manag.* **2021**, *239*, 114204. [CrossRef]